ACS Catalysis

Article

Copper-Gold Interactions Enhancing Formate Production from Electrochemical CO2 Reduction

Zixu Tao, Zishan Wu, Xiaolei Yuan, Yueshen Wu, and Hailiang Wang

ACS Catal., **Just Accepted Manuscript** • DOI: 10.1021/acscatal.9b03158 • Publication Date (Web): 21 Oct 2019

Just Accepted

is published by the American Chemical Society. 1155 Sixteenth Street N.W., Washington, DC 20036

Copper-Gold Interactions Enhancing Formate Production from Electrochemical CO_2 Reduction

Zixu Tao[1,2], Zishan Wu[1,2], Xiaolei Yuan[1,2,3], Yueshen Wu[1,2], Hailiang Wang*[1,2]

[1]Department of Chemistry, Yale University, New Haven, Connecticut 06520, United States

[2]Energy Sciences Institute, Yale University, West Haven, Connecticut 06516, United States

[3]School of Chemistry and Chemical Engineer, Nantong University, Nantong, Jiangsu, 226019, P. R. China

Abstract

Strong interactions between two different types of metal nanoparticles can dramatically change their electrocatalytic properties but are underexplored. Herein we show that interactions with Au can turn Cu, which by itself is neither selective nor active for electrochemical CO_2 reduction to formate, into a much improved electrocatalyst for the same reaction. Our Cu/Au catalyst produces formate in a significant yield at -0.4 V vs. the reversible hydrogen electrode in a near-neutral electrolyte and achieves a partial current density of 10.4 mA cm^{-2} and a Faradaic efficiency of 81% at -0.6 V, which is 15 times more active and 4 times more selective than the control Cu catalyst derived in the same way but without Au. Electrochemical and spectroscopic studies reveal that the metal-metal interactions in the Cu/Au catalyst lead to the disappearance of Au's characteristic electrocatalytic activity for reducing CO_2 and for oxidizing CO and to the stabilization of Cu^{1+} species on the Cu surface at CO_2 reduction potentials. Enhanced formate production from CO_2 electroreduction is now unlocked for the Cu-Au bimetallic system, implicating vast possibilities to improve electrocatalytic reactivity utilizing metal-metal interactions.

Keywords: CO_2 reduction, electrocatalysis, metal-metal interactions, copper-gold, formate-selective

*Corresponding author: Hailiang Wang. Email address: hailiang.wang@yale.edu

Artificial carbon fixation is a sustainable way to produce organic chemicals and to control the atmospheric CO_2 level, which could help alleviate the resource shortage and global warming issues[1]. In principle, the process involves reducing CO_2 with high-energy electrons from various sources, for example, from oxidation of H_2O or H_2S as in the natural processes of photosynthesis and chemosynthesis, or from H_2 as in the chemical industry[1]. Electrochemical CO_2 reduction, because of its mild and controllable working conditions and its compatibility with renewable energy sources, is a promising CO_2 fixation technique[2]. Formate, as a 2-electron reduction product from CO_2, is easily accessible and valuable[3]. Typical formate-selective CO_2 reduction electrocatalysts include some Group 14 and 15 metals, Pd and their alloys[4-9]. Sn, Pb and Bi are known for high formate selectivity (Faradaic efficiency, FE > 90%; all selectivity values are referenced to FE unless otherwise noted) but often times require potentials as negative as -1 V vs. the reversible hydrogen electrode (RHE; all potentials are referenced to the RHE unless otherwise noted)[10-16]; Pd can reduce CO_2 to formate with nearly zero overpotential, though the stability is seriously harmed by CO poisoning[9].

Among all the electrocatalysts for CO_2 reduction, Cu metal is perhaps the only one that can reduce CO_2 to many products including CO, formate, CH_4, C_2H_4 and alcohols across a wide potential range. However, Cu itself is not selective to any of these products, and the overall CO_2 conversion efficiency is often compromised by the hydrogen evolution reaction (HER). For example, a polycrystalline Cu mesh catalyzes CO_2 reduction to CH_4, C_2H_4, CO and some liquid products with a total FE < 70% at -0.96 V[17]; oxide-derived Cu can generate 33% formate and 40% CO at -0.55 V [18]. Various approaches have been taken to improve the selectivity and activity toward a single product[19-24]. For example, S-modified Cu nanoparticles achieved 80% formate at -0.8 V[20]; Cu foil treated with O_2 plasma produced 60% ethylene at -0.9 V[24]; Oxide-derived Cu nanowires on Cu mesh were 61.8% selective for producing CO at -0.4 V[25].

Metal-metal interactions play important roles in electrocatalysis. For example, the HER activity of Pd-based bimetallic systems was enhanced by optimizing the H adsorption energy via the interactions between the Pd overlayer and the metal substrate[26]. Research on Pt_3M (M=Ni, Co, Fe, Ti, V) demonstrated the effects of alloying on surface adsorbates and electrocatalytic O_2 reduction[27]. More recently, bimetallic electrocatalyst systems have been studied for CO_2 reduction[28-31]. A study of Au-coated Cu foil revealed that CO spillover from Au to Cu surface activates CO_2 reduction to ethanol and

*Corresponding author: Hailiang Wang. Email address: hailiang.wang@yale.edu

n-propanol at lower overpotentials[21]. A $CuSn_3$ material exhibited high formate selectivity (95%) at -0.5 V vs. RHE[32]. Our previous studies also demonstrated metal-metal interactions tuning CO_2 reduction catalysis: Pd on polycrystalline Cu induced continuous surface reconstruction and stabilized the CH_4/C_2H_4 production by Cu[17]; a single Pb-Pd electrocatalyst showed bifunctional activity for CO_2-formate interconversion due to reversible reconstruction under controlled electrochemical conditions[33]. Despite these progresses, it remains interesting and challenging to discover new metal-metal interactions leading to more desirable catalytic properties.

Herein, we report a new phenomenon of metal-metal interactions between Cu and Au, where the Au acts as a promoter to the Cu catalyzing electrochemical CO_2 reduction to formate (Figure 1). Our Cu/Au catalyst derived from a physical mixture of CuO and Au nanoparticles is able to produce formate in a significant yield at -0.4 V vs. RHE. Compared to CuO-derived Cu, it shows 15 times enhanced formate production, with the partial current density increased from 0.67 to 10.4 mA cm^{-2} and the FE elevated to over 80% at -0.6 V. This represents the most active CO_2-to-formate electrocatalyst with Cu as the primary component. The chemical states and properties of the surface Au and Cu sites are substantially modified as a result of the metal-metal interactions. The originally CO-selective Au nanoparticles are fully deactivated from producing CO; their characteristic electrochemical CO oxidation behavior is also absent. In addition, the interactions render more Cu^{1+} sites under the CO_2 reduction conditions, which may be related to the higher selectivity and activity for formate production.

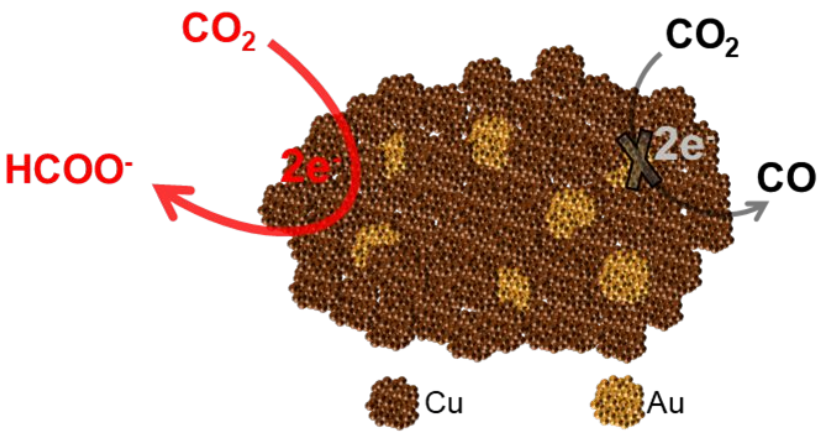

Figure 1. Schematic illustration of CO_2 reduction on the Cu/Au catalyst. The metal-metal interactions promote formate production on Cu and deactivate CO formation on Au.

The CuO and Au nanoparticles were synthesized separately following previously published

*Corresponding author: Hailiang Wang. Email address: hailiang.wang@yale.edu

methods with slight modifications (see Supporting Information, SI)[34-35]. Their X-ray diffraction (XRD) patterns (Figure S1a) match well with CuO (ICSD # 69758) and Au (ICSD # 44362), respectively. The CuO and Au nanoparticles have average sizes of 8 nm and 7 nm, respectively, as confirmed by the broadened diffraction peaks and the electron microscopy images (Figure S1b, c). Loaded on carbon fiber paper and tested in CO_2-saturated 0.5 M $KHCO_3$ aqueous electrolyte, the Au nanoparticles show high selectivity (> 80% FE) for CO between -0.5 V and -0.7 V (Figure S2a, b), which agrees with previously published results on Au nanoparticle electrocatalysts[36]. The CuO nanoparticles, which were electrochemically reduced to Cu metal prior to the CO_2 reduction measurement[18], exhibit potential-dependent selectivity changes characteristic for Cu (Figure 2a)[37]. Between -0.4 V and -0.6 V, H_2 and CO account for nearly all the reduction current. As the working electrode potential is switched stepwise to the more negative direction, C_2H_4 and CH_4 emerge in sequence. Liquid products are generated between -0.6 V and -1.0 V, as implied by the < 100% total FE of all the gas products. More than 40% of the electrons go to the HER across the entire potential range.

The Cu/Au catalyst was prepared by loading a mixture of the CuO and Au nanoparticles (8:1 mass ratio) on a carbon fiber paper electrode followed by an electrochemical pre-reduction. Compared to the Cu catalyst, this catalyst shows comparable partial current densities (Figure S3) but much lower FEs (Figure 2b) for H_2 and CO in the potential range between -0.4 V and -0.8 V. At -0.6 V, FE (H_2) and FE (CO) are 21.8% and 3.5%, respectively, indicating significant conversion of CO_2 to liquid product(s). To accumulate and quantify the liquid product(s), CO_2 reduction electrolysis was performed at -0.6 V. Formate was detected as the only product in the electrolyte (Figure S4). The Cu/Au catalyst shows an 81% selectivity for formate with a partial current density of 10.4 mA cm^{-2}. Compared to Cu, which exhibits a FE (formate) of 19% and a partial current density of 0.67 mA cm^{-2} at -0.6 V, the Cu/Au catalyst is 4 times higher in selectivity and 15 times higher in activity (i.e. current density) for reducing CO_2 to formate. The onset potential for formate production is at least 200 mV more positive (Figure 1a, b). In terms of overpotential, selectivity and reaction rate, this Cu/Au catalyst is competitive among formate-selective CO_2 reduction electrocatalysts (Table S1). Among all catalysts with Cu as the primary component, it is arguably the most active one reported to date. This is very different from previously reported Cu-Au bimetallic alloy nanoparticles where CO_2 reduction to CO was optimized while formate production remained at <5% FE, implying totally different metal-metal interactions in these two

*Corresponding author: Hailiang Wang. Email address: hailiang.wang@yale.edu

systems[38]. As the Cu/Au ratio is varied (with CuO/Au mixing ratios of 16:1 and 4:1, denoted as Cu/Au-A and Cu/Au-B, respectively), the FE of formate and its partial current density both change but remain much higher compared to those for the pure Cu catalyst (Figure 2c, d), supporting the positive effects of the Cu-Au interactions. In a 4-hour long electrolysis at -0.6 V, the Cu catalyst only maintained a total current density of 3.6 mA cm^{-2} with an averaged formate FE of 19% (Figure 2e). In contrast, 12 mA cm^{-2} with 79% formate selectivity was measured for the Cu/Au catalyst (Figure 2f).

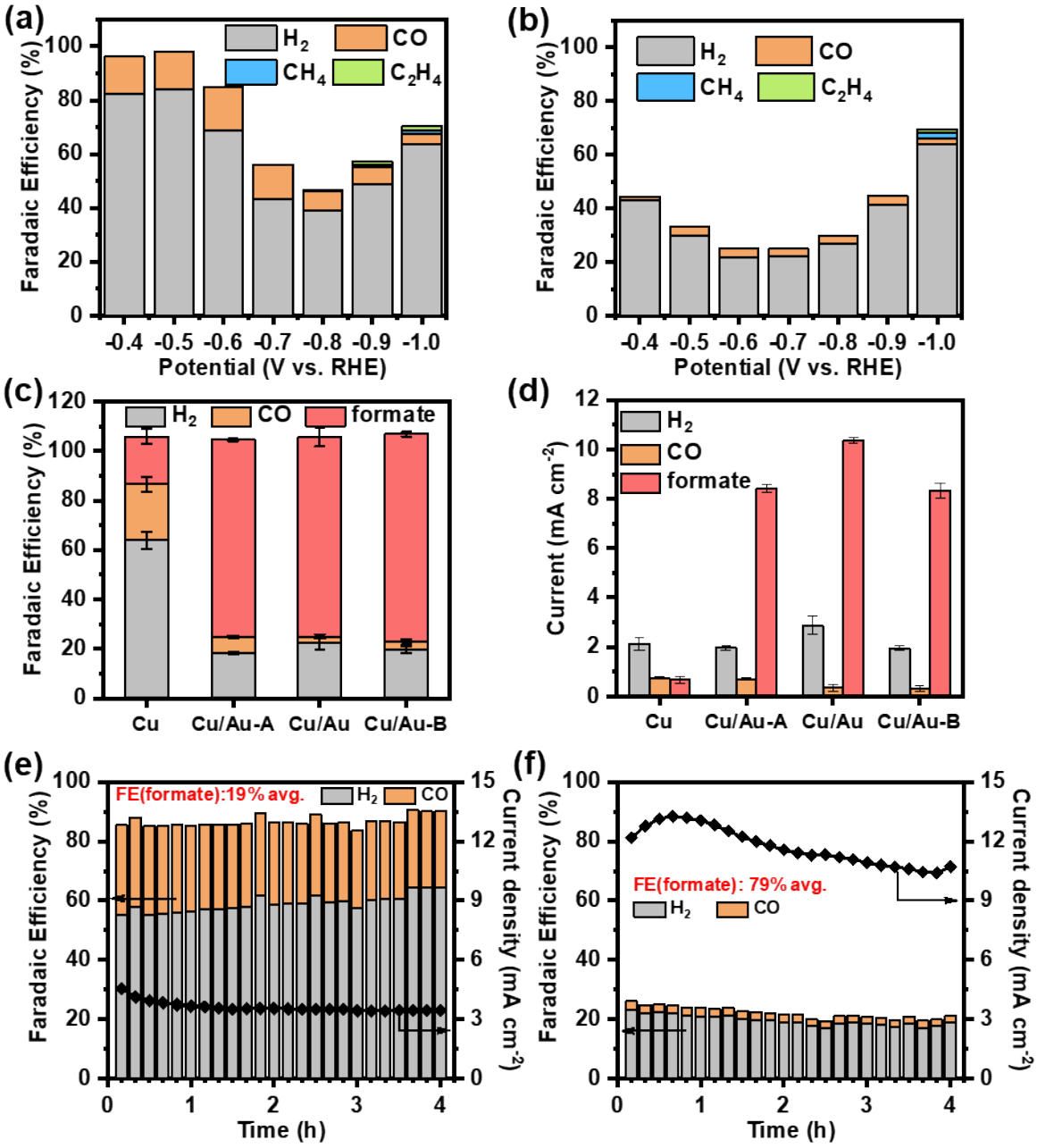

Figure 2. CO_2 reduction performance of the Cu/Au catalyst in CO_2-saturated 0.5 M $KHCO_3$. (a-b): Potential-dependent gas-phase product distribution for (a) Cu and (b) Cu/Au. (c-d): (c) FE distribution and (d) partial

*Corresponding author: Hailiang Wang. Email address: hailiang.wang@yale.edu

current densities of products for CO_2 reduction catalyzed by Cu, Cu/Au, Cu/Au-A and Cu/Au-B at -0.6 V. (e-f): 4-hour stability test for CO_2 reduction catalyzed by (e) Cu and (f) Cu/Au at -0.6 V. The average formate FEs were quantified after CO_2 reduction electrolysis.

To understand the origins of the unprecedented enhancement in electrocatalytic activity and selectivity of Cu by Au for CO_2 reduction to formate, we performed structural characterizations for the Cu/Au catalyst after the pre-reduction step. XRD shows that it is a mixed phase of Cu and Au without forming any Cu-Au alloy (Figure S5a). The catalyst manifests a morphology of coalesced particles with Au nanoparticles distributed in the Cu matrix reduced from CuO (Figure S5b, d-f), which is different from the original CuO and Au nanoparticles. The bulk Cu:Au atomic ratio was measured to be 95:5 (Figure S5c). X-ray photoelectron spectroscopy (XPS) depth profiling indicates that the two elements co-exist on the surface (Figure S5g). Both the microstructure and the electrochemical surface areas of the Cu/Au catalyst are similar to the Cu catalyst (Figure S6), implying that the CuO reduction process is not altered by the presence of the Au nanoparticles.

Au is well known for its electrocatalytic activity for selective CO_2 reduction to CO. However, in our Cu/Au catalyst, the Au component does not manifest its intrinsic activity. We thereby propose that the surface Au sites are deactivated because of their interactions with Cu. This hypothesis is further supported by our electrochemical CO oxidation studies. Measured in 0.5 M aqueous $KHCO_3$, the Au nanoparticles clearly exhibit the characteristic activity of Au metal toward electrochemical oxidation of CO at around 1.1 V in both the forward and reverse scans (Figure 3a)[39]. In contrast, this CO oxidation behavior is absent for the Cu/Au catalyst despite the presence of the redox waves associated with Cu (Figure 3b). The other Cu/Au catalysts with different Cu:Au ratios do not show CO oxidation activity either (Figure S7), confirming that the deactivation of Au is caused by the presence of the Cu component in the catalyst structure. Note that the Au nanoparticles were synthesized in the presence of cetyltrimethylammonium bromide. The surface ligand may have played a role in the metal-metal interactions[40], which warrants further investigation.

*Corresponding author: Hailiang Wang. Email address: hailiang.wang@yale.edu

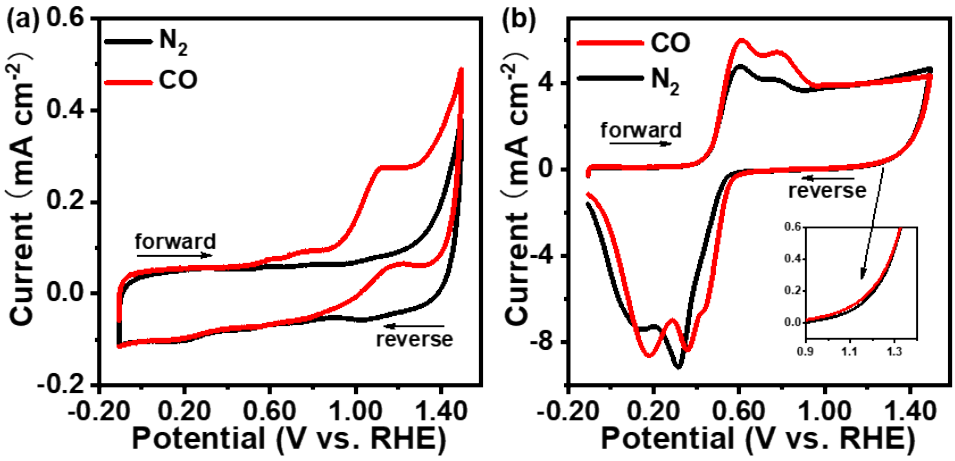

Figure 3. Cyclic voltammograms of (a) Au nanoparticles and (b) the Cu/Au catalyst in 0.5 M $KHCO_3$ saturated with N_2 or CO.

Quasi-in-situ XPS[41-43] was performed to study the surface structure of the Cu/Au catalyst. The surface Au sites are in the Au^0 state, as evidenced by the binding energy of the Au 4f electrons (Figure 4a). The binding energy of the Cu 2p electrons and the absence of their satellite peaks demonstrate that the Cu^{2+} from the original CuO nanoparticles has been fully reduced (Figure 4b). Given that Cu^{1+} and Cu^0 cannot be distinguished in the Cu 2p XPS spectrum (Figure S8), we acquired the Cu LMM Auger spectrum to analyze the oxidation state. While the surface of the Cu catalyst is dominated by Cu^0, the Cu/Au catalyst contains a significant number of Cu^{1+} sites (Figure 4c). Further experiments show that the oxidation states of the Au and Cu sites are retained after long-term electrolysis (Figure S9). These results suggest that the Cu-Au metal-metal interactions stabilize Cu^{1+} on the surface under reducing potentials, which is likely related to the enhanced performance for CO_2 reduction[18, 44].

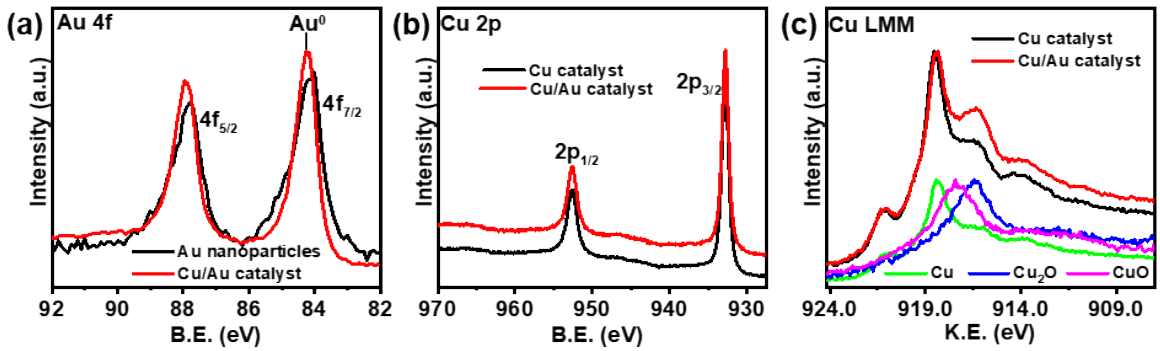

Figure 4. (a) Au 4f XPS spectra of the Cu/Au catalyst and Au nanoparticles. (b) Cu 2p XPS spectra and (c) Cu LMM auger spectra of the Cu/Au and Cu catalysts.

*Corresponding author: Hailiang Wang. Email address: hailiang.wang@yale.edu

In summary, we have developed a formate-selective CO_2 reduction electrocatalyst based on an intimate mixture of Cu and Au nanoparticles. The metal-metal interactions make the Cu 15 times more active and 4 times more selective toward CO_2 conversion to formate; the Au is deactivated for converting CO_2 to CO. These findings highlight the promise of utilizing inter-nanoparticle metal-metal interactions to improve CO_2 reduction electrocatalysis.

Supporting Information

Experimental details and additional figures.

Acknowledgement

This work was supported by the National Science Foundation (Grant CHE-1651717)

References

1. Artz, J.; Muller, T. E.; Thenert, K.; Kleinekorte, J.; Meys, R.; Sternberg, A.; Bardow, A.; Leitner, W., Sustainable Conversion of Carbon Dioxide: An Integrated Review of Catalysis and Life Cycle Assessment. *Chem Rev* **2018,** *118*, 434-504.
2. Duan, X.; Xu, J.; Wei, Z.; Ma, J.; Guo, S.; Wang, S.; Liu, H.; Dou, S., Metal-Free Carbon Materials for CO_2 Electrochemical Reduction. *Adv Mater* **2017,** *29*, 1701784.
3. Yoo, J. S.; Christensen, R.; Vegge, T.; Norskov, J. K.; Studt, F., Theoretical Insight into the Trends that Guide the Electrochemical Reduction of Carbon Dioxide to Formic Acid. *ChemSusChem* **2016,** *9*, 358-363.
4. Klinkova, A.; De Luna, P.; Dinh, C. T.; Voznyy, O.; Larin, E. M.; Kumacheva, E.; Sargent, E. H., Rational Design of Efficient Palladium Catalysts for Electroreduction of Carbon Dioxide to Formate. *Acs Catal* **2016,** *6*, 8115-8120.
5. Rahaman, M.; Dutta, A.; Broekmann, P., Size-Dependent Activity of Palladium Nanoparticles: Efficient Conversion of CO_2 into Formate at Low Overpotentials. *ChemSusChem* **2017,** *10*, 1733-1741.
6. Bai, X.; Chen, W.; Zhao, C.; Li, S.; Song, Y.; Ge, R.; Wei, W.; Sun, Y., Exclusive Formation of Formic Acid from CO_2 Electroreduction by a Tunable Pd-Sn Alloy. *Angew Chem Int Ed Engl* **2017,** *56*, 12219-12223.
7. Gao, D. F.; Zhou, H.; Cai, F.; Wang, D. N.; Hu, Y. F.; Jiang, B.; Cai, W. B.; Chen, X. Q.; Si, R.; Yang, F.; Miao, S.; Wang, J. G.; Wang, G. X.; Bao, X. H., Switchable CO_2 Electroreduction via Engineering Active Phases of Pd Nanoparticles. *Nano Res* **2017,** *10*, 2181-2191.
8. Gao, D. F.; Zhou, H.; Cai, F.; Wang, J. G.; Wang, G. X.; Bao, X. H., Pd-Containing Nanostructures for Electrochemical CO_2 Reduction Reaction. *Acs Catal* **2018,** *8*, 1510-1519.
9. Min, X.; Kanan, M. W., Pd-Catalyzed Electrohydrogenation of Carbon Dioxide to Formate: High Mass Activity at Low Overpotential and Identification of the Deactivation Pathway. *J Am Chem Soc* **2015,** *137*, 4701-4708.
10. Han, N.; Wang, Y.; Yang, H.; Deng, J.; Wu, J.; Li, Y.; Li, Y., Ultrathin Bismuth Nanosheets from In-Situ Topotactic Transformation for Selective Electrocatalytic CO_2 Reduction to Formate. *Nat Commun* **2018,** *9*, 1320.
11. Wang, J.; Wang, H.; Han, Z. Z.; Han, J. Y., Electrodeposited Porous Pb Electrode with Improved

*Corresponding author: Hailiang Wang. Email address: hailiang.wang@yale.edu

Electrocatalytic Performance for the Electroreduction of CO_2 to Formic Acid. *Front Chem Sci Eng* **2015,** *9*, 57-63.

12. Back, S.; Kim, J. H.; Kim, Y. T.; Jung, Y., On the Mechanism of High Product Selectivity for HCOOH Using Pb in CO_2 Electroreduction. *Phys Chem Chem Phys* **2016,** *18*, 9652-9657.

13. Lee, C. H.; Kanan, M. W., Controlling H^+ vs CO_2 Reduction Selectivity on Pb Electrodes. *Acs Catal* **2015,** *5*, 465-469.

14. Li, A.; Wang, H.; Han, J.; Liu, L., Preparation of a Pb Loaded Gas Diffusion Electrode and its Application to CO_2 Electroreduction. *Front Chem Sci Eng* **2012,** *6*, 381-388.

15. Zhang, S.; Kang, P.; Meyer, T. J., Nanostructured Tin Catalysts for Selective Electrochemical Reduction of Carbon Dioxide to Formate. *J Am Chem Soc* **2014,** *136*, 1734-1737.

16. Choi, S. Y.; Jeong, S. K.; Kim, H. J.; Baek, I.-H.; Park, K. T., Electrochemical Reduction of Carbon Dioxide to Formate on Tin–Lead Alloys. *ACS Sustainable Chemistry & Engineering* **2016,** *4*, 1311-1318.

17. Weng, Z.; Zhang, X.; Wu, Y.; Huo, S.; Jiang, J.; Liu, W.; He, G.; Liang, Y.; Wang, H., Self-Cleaning Catalyst Electrodes for Stabilized CO_2 Reduction to Hydrocarbons. *Angew Chem Int Ed Engl* **2017,** *56*, 13135-13139.

18. Li, C. W.; Kanan, M. W., CO_2 Reduction at Low Overpotential on Cu Electrodes Resulting from the Reduction of Thick Cu_2O Films. *J Am Chem Soc* **2012,** *134*, 7231-7234.

19. Le Duff, C. S.; Lawrence, M. J.; Rodriguez, P., Role of the Adsorbed Oxygen Species in the Selective Electrochemical Reduction of CO_2 to Alcohols and Carbonyls on Copper Electrodes. *Angew Chem Int Ed Engl* **2017,** *56*, 12919-12924.

20. Shinagawa, T.; Larrazabal, G. O.; Martin, A. J.; Krumeich, F.; Perez-Ramirez, J., Sulfur-Modified Copper Catalysts for the Electrochemical Reduction of Carbon Dioxide to Formate. *Acs Catal* **2018,** *8*, 837-844.

21. Morales-Guio, C. G.; Cave, E. R.; Nitopi, S. A.; Feaster, J. T.; Wang, L.; Kuhl, K. P.; Jackson, A.; Johnson, N. C.; Abram, D. N.; Hatsukade, T.; Hahn, C.; Jaramillo, T. F., Improved CO_2 Reduction Activity Towards C_{2+} Alcohols on a Tandem Gold on Copper Electrocatalyst. *Nat Catal* **2018,** *1*, 764-771.

22. Peng, Y.; Wu, T.; Sun, L.; Nsanzimana, J. M. V.; Fisher, A. C.; Wang, X., Selective Electrochemical Reduction of CO_2 to Ethylene on Nanopores-Modified Copper Electrodes in Aqueous Solution. *ACS Appl Mater Interfaces* **2017,** *9*, 32782-32789.

23. Li, Y.; Cui, F.; Ross, M. B.; Kim, D.; Sun, Y.; Yang, P., Structure-Sensitive CO_2 Electroreduction to Hydrocarbons on Ultrathin 5-fold Twinned Copper Nanowires. *Nano Lett* **2017,** *17*, 1312-1317.

24. Mistry, H.; Varela, A. S.; Bonifacio, C. S.; Zegkinoglou, I.; Sinev, I.; Choi, Y.-W.; Kisslinger, K.; Stach, E. A.; Yang, J. C.; Strasser, P.; Cuenya, B. R., Highly Selective Plasma-Activated Copper Catalysts for Carbon Dioxide Reduction to Ethylene. *Nature Communications* **2016,** *7*, 12123.

25. Raciti, D.; Livi, K. J.; Wang, C., Highly Dense Cu Nanowires for Low-Overpotential CO_2 Reduction. *Nano Lett* **2015,** *15*, 6829-6835.

26. Greeley, J.; Norskov, J. K.; Kibler, L. A.; El-Aziz, A. M.; Kolb, D. M., Hydrogen Evolution over Bimetallic Systems: Understanding the Trends. *Chemphyschem* **2006,** *7*, 1032-1035.

27. Stamenkovic, V. R.; Mun, B. S.; Arenz, M.; Mayrhofer, K. J.; Lucas, C. A.; Wang, G.; Ross, P. N.; Markovic, N. M., Trends in Electrocatalysis on Extended and Nanoscale Pt-Bimetallic Alloy Surfaces. *Nat Mater* **2007,** *6*, 241-247.

28. Lee, C. W.; Yang, K. D.; Nam, D. H.; Jang, J. H.; Cho, N. H.; Im, S. W.; Nam, K. T., Defining a Materials Database for the Design of Copper Binary Alloy Catalysts for Electrochemical CO_2 Conversion. *Adv Mater* **2018,** *30*, 1704717.

29. Vickers, J. W.; Alfonso, D.; Kauffman, D. R., Electrochemical Carbon Dioxide Reduction at Nanostructured Gold, Copper, and Alloy Materials. *Energy Technol-Ger* **2017,** *5*, 775-795.

*Corresponding author: Hailiang Wang. Email address: hailiang.wang@yale.edu

30. Xu, Z.; Lai, E.; Shao-Horn, Y.; Hamad-Schifferli, K., Compositional Dependence of the Stability of AuCu alloy nanoparticles. *Chem Commun (Camb)* **2012,** *48*, 5626-5628.

31. Christophe, J.; Doneux, T.; Buess-Herman, C., Electroreduction of Carbon Dioxide on Copper-Based Electrodes: Activity of Copper Single Crystals and Copper–Gold Alloys. *Electrocatalysis* **2012,** *3*, 139-146.

32. Zheng, X.; Ji, Y.; Tang, J.; Wang, J.; Liu, B.; Steinrück, H.-G.; Lim, K.; Li, Y.; Toney, M. F.; Chan, K.; Cui, Y., Theory-Guided Sn/Cu Alloying for Efficient CO_2 Electroreduction at Low Overpotentials. *Nat Catal* **2018,** *2*, 55-61.

33. Lu, X.; Wu, Y.; Yuan, X.; Wang, H., An Integrated CO_2 Electrolyzer and Formate Fuel Cell Enabled by a Reversibly Restructuring Pb-Pd Bimetallic Catalyst. *Angew Chem Int Ed Engl* **2019,** *58*, 4031-4035.

34. Zhu, J. W.; Bi, H. P.; Wang, Y. P.; Wang, X.; Yang, X. J.; Lu, L., CuO Nanocrystals with Controllable Shapes Grown from Solution without Any Surfactants. *Mater Chem Phys* **2008,** *109*, 34-38.

35. Jana, N. R.; Gearheart, L.; Murphy, C. J., Seeding Growth for Size Control of 5−40 nm Diameter Gold Nanoparticles. *Langmuir* **2001,** *17*, 6782-6786.

36. Zhu, W.; Michalsky, R.; Metin, O.; Lv, H.; Guo, S.; Wright, C. J.; Sun, X.; Peterson, A. A.; Sun, S., Monodisperse Au Nanoparticles for Selective Electrocatalytic Reduction of CO_2 to CO. *J Am Chem Soc* **2013,** *135*, 16833-16836.

37. Gattrell, M.; Gupta, N.; Co, A., A Review of the Aqueous Electrochemical Reduction of CO_2 to Hydrocarbons at Copper. *J Electroanal Chem* **2006,** *594*, 1-19.

38. Kim, D.; Resasco, J.; Yu, Y.; Asiri, A. M.; Yang, P., Synergistic Geometric and Electronic Effects for Electrochemical Reduction of Carbon Dioxide Using Gold–Copper Bimetallic Nanoparticles. *Nature Communications* **2014,** *5*, 4948 1-8.

39. Rodriguez, P.; Kwon, Y.; Koper, M. T., The Promoting Effect of Adsorbed Carbon Monoxide on the Oxidation of Alcohols on a Gold Catalyst. *Nat Chem* **2011,** *4*, 177-182.

40. Wu, Y.; Yuan, X.; Tao, Z.; Wang, H., Bifunctional Electrocatalysis for CO_2 Reduction via Surface Capping-Dependent Metal–Oxide Interactions. *Chemical Communications* **2019,** *55*, 8864-8867.

41. Wu, Z. S.; Li, X. L.; Liu, W.; Zhong, Y. R.; Gan, Q.; Li, X. M.; Wang, H. L., Materials Chemistry of Iron Phosphosulfide Nanoparticles: Synthesis, Solid State Chemistry, Surface Structure, and Electrocatalysis for the Hydrogen Evolution Reaction. *Acs Catal* **2017,** *7*, 4026-4032.

42. Gan, Q.; Wu, Z. S.; Li, X. L.; Liu, W.; Wang, H. L., Structure and Electrocatalytic Reactivity of Cobalt Phosphosulfide Nanomaterials. *Top Catal* **2018,** *61*, 958-964.

43. Wu, Z. S.; Huang, L.; Liu, H.; Wang, H. L., Element-Specific Restructuring of Anion- and Cation-Substituted Cobalt Phosphide Nanoparticles under Electrochemical Water-Splitting Conditions. *Acs Catal* **2019,** *9*, 2956-2961.

44. Reske, R.; Mistry, H.; Behafarid, F.; Roldan Cuenya, B.; Strasser, P., Particle Size Effects in the Catalytic Electroreduction of CO_2 on Cu Nanoparticles. *J Am Chem Soc* **2014,** *136*, 6978-6986.

*Corresponding author: Hailiang Wang. Email address: hailiang.wang@yale.edu

TOC graphic

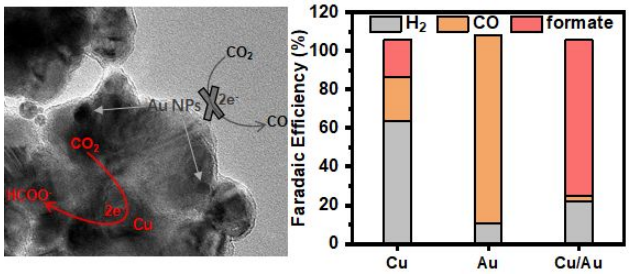

*Corresponding author: Hailiang Wang. Email address: hailiang.wang@yale.edu